DOI: 10.1002/ejoc.200600780

Stable Ion and Electrophilic Substitution (Nitration and Bromination) Study of A-Ring Substituted Phenanthrenes: Novel Carbocations and Substituted Derivatives; NMR, X-ray Analysis, and Comparative DNA Binding

Cédric Brulé,[a] Kenneth K. Laali,*[a] Takao Okazaki,[a] Tamara Musafia,[b] and William M. Baird[b]

Keywords: Persistent carbocations / NMR spectroscopy / Nitration and bromination / X-ray analysis / Comparative DNA binding study

Persistent carbocations were generated from five A-ring mono- and di-substituted phenanthrenes [3-OMe; 4-OMe, 1,3-bis(OMe), 2,4-bis(OMe), and 1,3-bis(Me)]. In all cases protonation occurs in the A-ring, *ortho*/*para* relative to methoxy or methyl substituent(s). Complete NMR assignments of the resulting carbocations are reported and their charge delocalization modes are discussed. Mild nitration (with 20–50 % aqueous HNO_3 at –10 °C or at room temp.) and bromination (NBS/MeCN/room temp.) of these substrates resulted in the synthesis of several novel mononitro-/dinitro- as well as monobromo/dibromo derivatives, including those with nitro or bromo substituent in the bay-region. Correspondence between the site of attack in low-temperature protonation study and nitro substitution in ambient mild nitrations are examined. Complete NMR assignments for the new derivatives are reported as well as X-ray structures for 2,4-dimethoxy-1-nitro- and 1,3-dimethyl-4-nitrophenanthrenes. A comparative DNA binding study with MCF cells on three of the synthesized mononitro and one dinitro derivative showed that 1,3-dimethyl-9-nitro- (nitro at the *meso* position), 3-methoxy-4-nitro- (nitro in bay-region), and 1,3-dimethoxy-4,9-dinitrophenanthrenes (nitro in both *meso* and bay-regions) formed DNA adducts.

Introduction

The phenanthrene (Ph) skeleton (Figure 1) is an important building block of alternant polyarenes. Its monobenzannelated derivatives, in particular chrysene, benz[*a*]-anthracene and benzo[*c*]phenanthrene have been extensively studied with regard to their bio-activity and for establishing structure–activity relationships.[1,2]

Whereas parent Ph itself is a noncarcinogen, some of its methylated derivatives are quite active.[3] In particular 1,4-DMPh and 1,3,4-TMPh were shown to be tumorigenic in bioassays.[3] The dihydrodiol precursors to the bay-region diol epoxides were suggested to be responsible for tumorigenic activity in the methylated phenanthrenes.[3] Depending on the substitution mode, nitrophenanthrenes are mutagenic, in particular those with the nitro group at C-3/C-6 were shown to be highly mutagenic.[4]

Earlier, a number of stable carbocations derived from methylated-Ph were generated in superacidic media and studied by NMR spectroscopy.[5,6] Stable phenanthrenium ions were also formed indirectly via the hindered olefin (*Z*)-

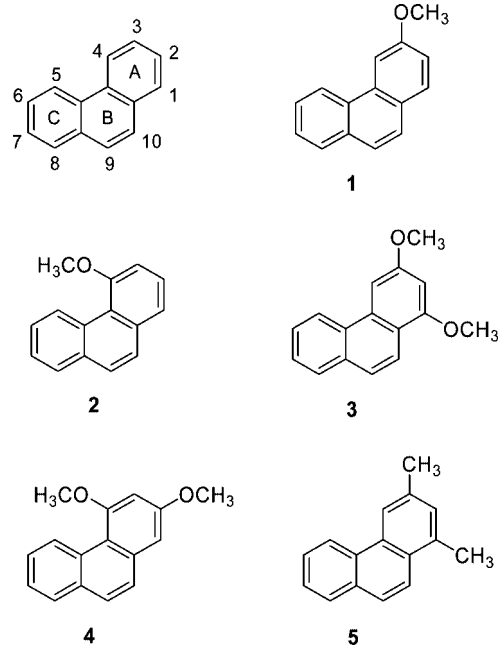

Figure 1. Studied A-ring substituted phenanthrenes.

[a] Department of Chemistry, Kent State University, Kent, OH 44242, USA
Fax: +1-330-6723816
E-mail: klaali@kent.edu
[b] Environmental and Molecular Toxicology Department, Oregon State University, Corvallis OR 97331, USA

Supporting information for this article is available on the WWW under http://www.eurjoc.org or from the author.

2,2,5,5-tetramethyl-3,4-diphenylhex-3-ene, by facial ring protonation and subsequent transannular cyclization.[7]

Previous stable ion studies of chrysenes and benzo[*c*]-phenanthrenes underscored the highly effective directive effect of a methoxy substituent, as well as its stabilizing effect in the resulting arenium ions.[8] The A-ring substituted methoxy- and methylphenanthrenes are interesting substrates for carbocation generation as possible models for electrophiles derived from 1,2-diol-3,4-epoxide. A recently reported flexible synthetic method involving $PtCl_2$-catalyzed cycloisomerization of *ortho*-alkynylated biphenyl derivatives provided access to the A-ring methoxy and methyl derivatives used in the present study (Figure 1).[9]

Results and Discussion

a) NMR Features in the Substrates

The ^1H and ^{13}C NMR spectra for the compounds **1**–**5** had previously been reported[9] without specific assignments. Complete NMR assignments were made in the present study by using 2D-NMR techniques. The spectroscopic data are summarized in Figure 2.

It can be seen that methoxy or methyl substitution at C-3 has a shielding effect on 4-H (compounds **1**, **3** and **5**), whereas substitution at C-4 results in significant deshielding at 5-H[10] (across the bay-region). In the ^{13}C NMR, the methoxy- and methyl-bearing quaternary carbon atoms are most deshielded. The protons of the methoxy group in the bay-region (as in **2** and **4**) are more deshielded relative to substitution in other positions in the A-ring (as in **1** and **3**).

b) Stable Ion Study in FSO_3H/SO_2ClF

Persistent phenanthrenium ions were generated according to the protocol described in the experimental section. They were fully characterized by NMR at low temperature.

Low-temperature protonation of **1** resulted in attack at C-4, generating the two carboxonium ions **1aH$^+$** and **1bH$^+$**, as distinct conformational isomers (in 2:1 ratio) at –65 °C (Scheme 1), whose relative assignment was established by NOE. Their relative ratio is consistent with the expectation that **1aH$^+$** conformer is sterically less crowded and hence lower in energy. By raising the temperature to –20 °C the two conformers converged into a single averaged carboxonium ion **1H$^+$** (Scheme 1). For specific NMR assignments of the carbocations see Figure 3. NOE interactions were observed in **1H$^+$** between the CH_2 protons and 5-H, between the OMe and 2-H and between 1-H and 10-H (*peri*), confirming the protonation site. Charge delocalization mode in **1H$^+$**, as well as in **1aH$^+$/1bH$^+$**, shows that positive charge resides in the A-ring (*ortho*/*para* to the protonation site), with limited delocalization into one other conjugated carbon in the B-ring (Figure 4).

Low-temperature protonation of compound **2**, bearing a methoxy group in the bay-region, led to **2H$^+$** by protonation at C-1 (*para* position) (Scheme 1). A minor unidentified side-product (<15%) corresponding to either protonation at a different site or another conformational isomer was also present. The most deshielded carbon resonance in **2H$^+$** is that of *C*–OMe at δ = 190.4 ppm (Figure 3). Interestingly, 5-H in **2H$^+$** is shielded relative to that in **2**, indicating that the bay-region deshielding effect is diminished in the

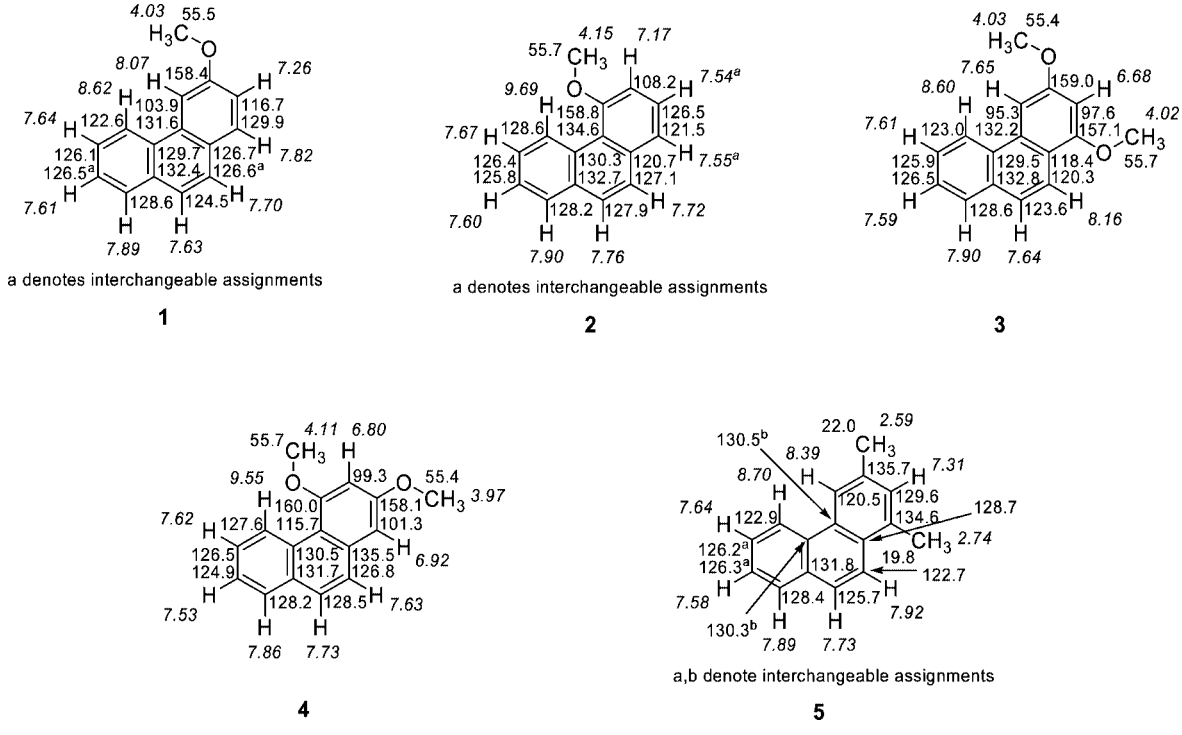

Figure 2. ^1H and ^{13}C NMR assignments for the studied substituted phenanthrenes.

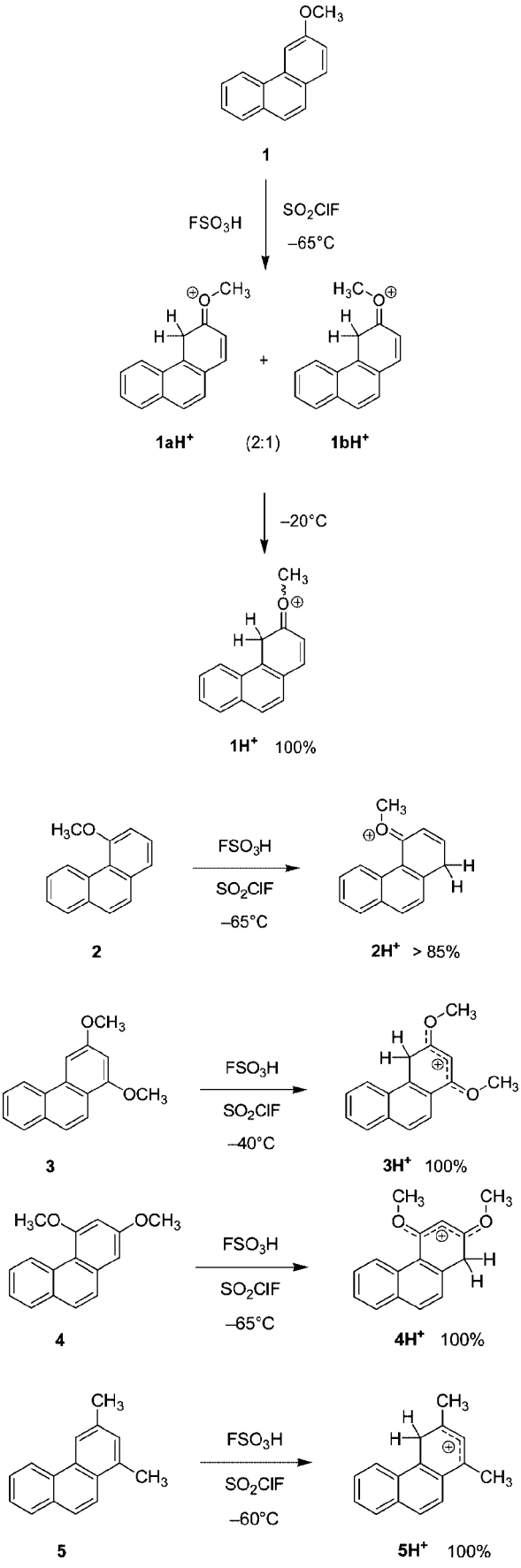

Scheme 1.

carbocation due to OMe conformational change in the carboxonium ion.

For **2H$^+$**, NOE effects were detected for OMe with both 3-H and 5-H, for CH_2 with 2-H and 10-H, confirming C-1 as protonation site. In addition, NOEs were also detected for the following pairs of protons 2-H/3-H, 9-H/10-H, 9-H/8-H, and 7-H/8-H. Positive charge in **2H$^+$** is delocalized into the A-ring (*ortho*/*para* to CH_2) plus one conjugated carbon in the B-ring (Figure 4).

Protonation of the 1,3-dimethoxy-substituted derivative **3**, led to exclusive formation of **3H$^+$** (Scheme 1). Highly deshielded methoxy groups in **3H$^+$** reflect strong carboxonium ion character in this carbocation (Figure 3). Bay-region protonation leads to an upfield shift of 5-H. NOE was observed for CH_2/5-H, confirming C-4 as protonation site. Charge delocalization maps for **3H$^+$** and **1H$^+$** are rather similar (Figure 4).

Low-temperature protonation of the 2,4-dimethoxy derivative **4** led to exclusive formation of **4H$^+$** (Scheme 1). As in the previous example, the highly deshielded methoxy groups are indicative of strong carboxonium ion character in **4H$^+$** (Figure 3). NOE studies showed that both OMe groups exhibited interactions with 3-H (no NOE detected between CH_2 and OMe or between OMe and 5-H). This sets the conformation of **4H$^+$**, as shown in Scheme 1. NOE effects were also detected for several other pairs of protons including CH_2/10-H. Charge delocalization mode in **4H$^+$** is analogous to **2H$^+$** (Figure 4).

Low-temperature protonation of the dimethyl derivative **5** led to clean formation of the carbocation **5H$^+$** by protonation at C-4 (Scheme 1 and Figure 3). NOE effects were observed between CH_2 and 5-H. Both methyl groups exhibited NOE with 2-H. Charge-delocalization pattern in the arenium ion indicates strong charge localization in the A-ring similar to **3H$^+$** (Figure 4).

c) Electrophilic Nitration and Bromination (Scheme 2)

Using nitration and bromination as prototypic reactions, electrophilic substitution chemistry of the compounds **1-5** was investigated. Regioselectivity in nitration was of particular interest for comparison with the protonation sites in the carbocations.

Compound **1** was readily nitrated under very mild conditions by reaction with 30% HNO_3 at –10 °C in a short period of time to give two isomeric mono-nitro products **1aNO$_2$** and **1bNO$_2$** by substitution at C-9 (*meso* position or K-region) and at C-4 (bay-region), as major and minor products, respectively. Nitro substitution at C-9 in **1aNO$_2$** was confirmed by NOE interactions between 10-H and 1-H. The nitro group at C-9 exerts a strong deshielding effect on 10-H and 8-H. Whereas nitro substitution at C-4 (**1bNO$_2$**) has a deshielding effect on 1-H (*para*), it produces a shielding effect at 5-H, which is consistent with nitro group buttressing, and decreasing the bay-region steric crowding.

Compound **1** reacted with NBS in MeCN at room temp. to furnish only the 9-bromo derivative **1Br** in good yield.

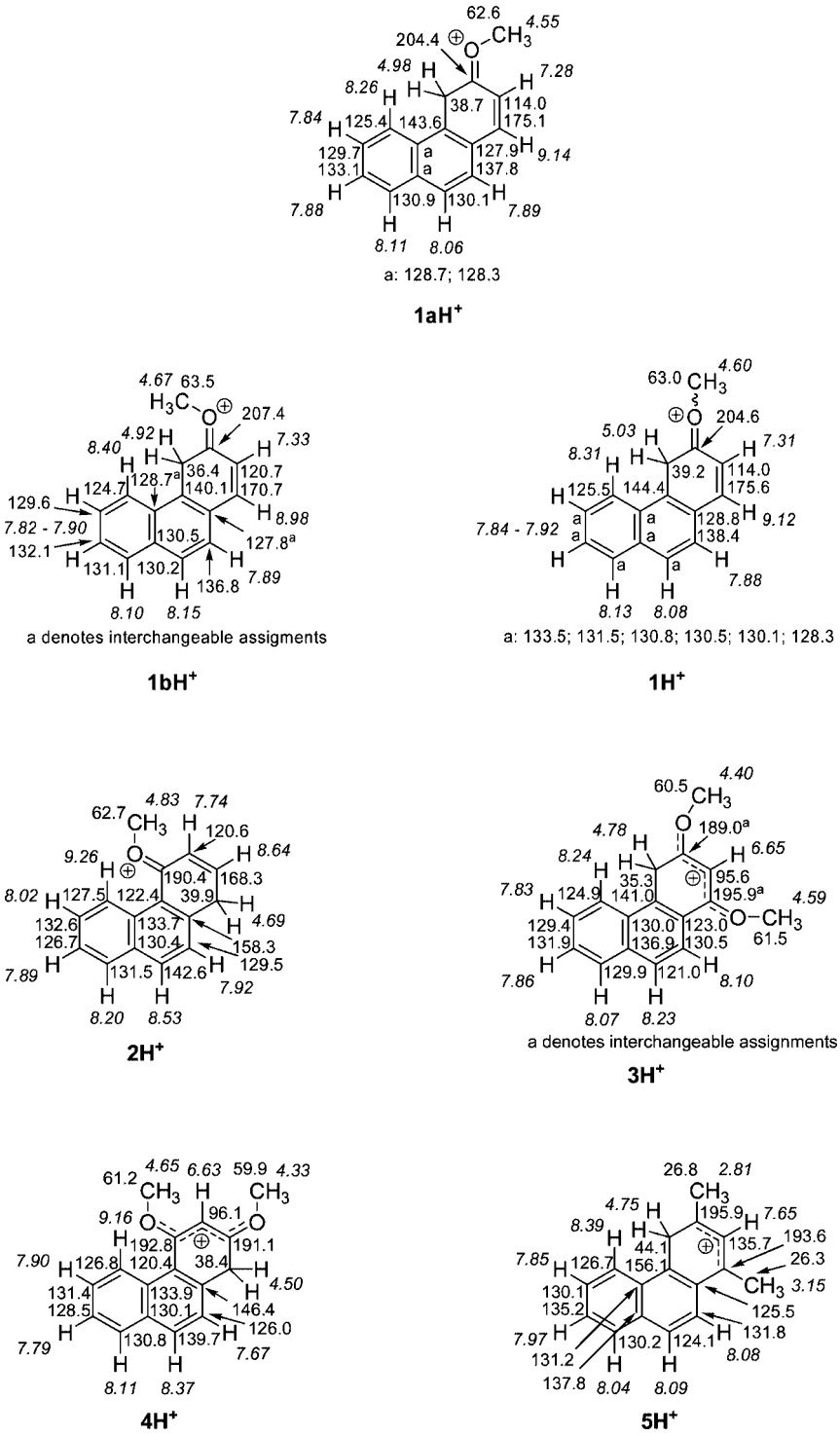

Figure 3. ^{1}H and ^{13}C NMR assignments for the phenanthrenium ions.

Br substitution at C-9 has a deshielding effect on both 10-H and 8-H, but less so as compared to **1aNO$_2$**. These findings are in agreement with low-temperature protonation study, and further demonstrate that increasing the size of the electrophile renders substitution at C-4 unfavorable.

Protic nitration of compound **2** with HNO_3 (50%)/AcOH at room temp., yielded a mononitro (**2aNO$_2$**) and a dinitro product (**2bNO$_2$**) in rather similar ratios. Surprisingly, a mononitro derivative with the nitro group at C-4 (**2cNO$_2$**) was not observed in this case (see further). In the 1,3-dinitro derivative **2bNO$_2$**, 5-H exhibits NOE with both OMe and 6-H. By repeating the nitration under milder conditions, it was possible to suppress dinitration and obtain two regioisomeric mono-nitro products **2cNO$_2$** (major) and **2aNO$_2$** (minor) in a good overall yield, corresponding to electrophilic substitution at the *para* and *ortho* position to

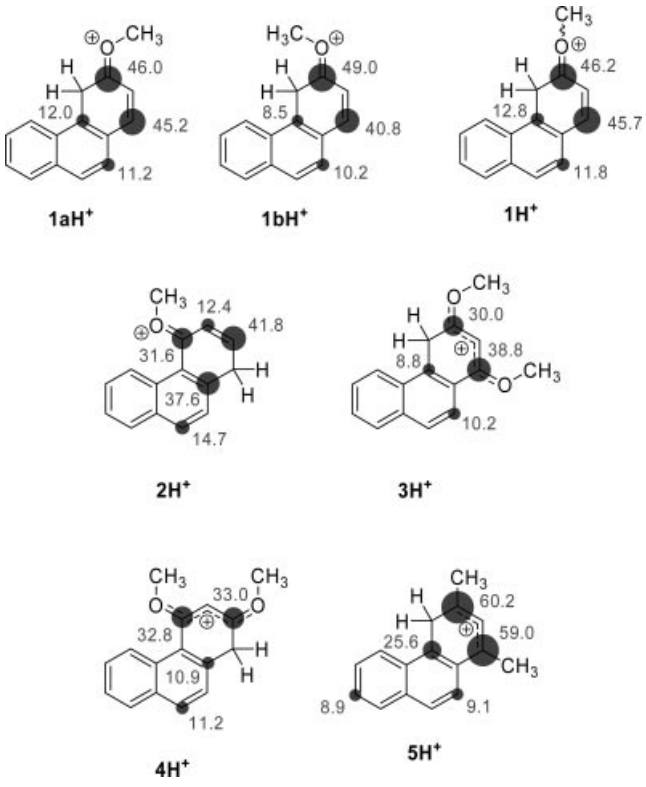

Figure 4. $\Delta\delta^{13}$C between protonated and neutral species (threshold 8 ppm).

methoxy. It is interesting to note that under stable ion conditions (Scheme 1), only the C-1 protonated carbocation was observed (*para*).

Nitration of compound **3** under standard conditions led to the 4,9-dinitrated product **3NO$_2$** in moderate yield.

Bromination of **3** with NBS/MeCN resulted in a 7:3 mixture of the mono and dibromo derivatives **3aBr** and **3bBr**, respectively, in over 90% yield. The regiochemistry of the substitution was determined by NOE irradiations for both **3aBr** and **3bBr** as a mixture. The *ortho*/*peri* deshielding effect of bromine at the *meso* position is evident in both compounds. A notable feature in **3bBr** (bromine at bay-region) is the highly deshielded 5-H (almost at δ = 10 ppm!). The electrophilic reactivity patterns in **3** in protonation, nitration and bromination are comparable to those in **1**.

To prevent overnitration in the case of **4**, very mild conditions were used (20% aqueous HNO_3 at –10 °C). This resulted in clean isolation of the mononitro derivative **4NO$_2$**. Thus compound **4** exhibited similar regioselectivity in protonation and in mild nitration.

Suitable crystals could be grown and the X-ray structure of **4NO$_2$** was determined (Figure 5 and experimental part). It shows that the two methoxy groups are facing each other, probably to minimize steric interaction with the nitro group on one side and 5-H on the other side (this fits in with the suggested solution conformation based on NOE in the case of **4H$^+$**, see before). The PAH core is planar, but the nitro group is buttressed with a buttressing angle of 68.5°.

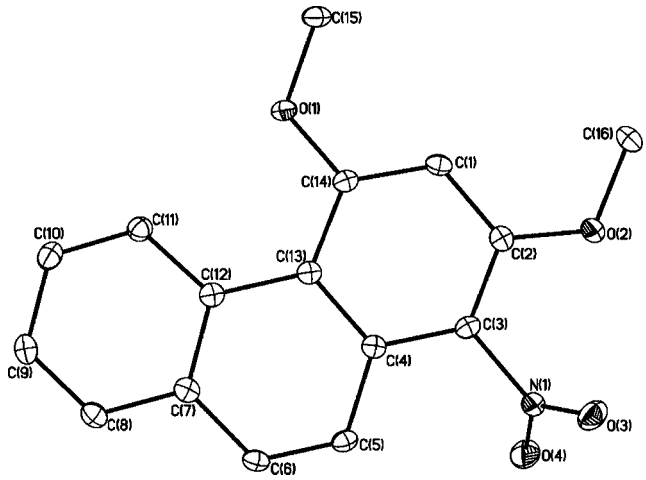

Figure 5. Thermal ellipsoid plot of **4NO$_2$**. Ellipsoids are drawn at the 30% level.

Nitration of compound **5** was performed under two sets of conditions with 50% aqueous HNO_3/AcOH at room temp. and with 40% HNO_3/AcOH at –10 °C. In both cases, two regioisomeric mono-nitrated derivatives **5aNO$_2$** and **5bNO$_2$** were isolated, resulting from nitration at the bay-region and at the *meso* position respectively. The proportion of the 9-NO_2 derivative was substantially higher under milder conditions (Scheme 2). Whereas nitration at the *meso* position (**5bNO$_2$**) resulted in pronounced *ortho*/*peri* deshielding (10-H/8-H), nitration at the bay-region (**5aNO$_2$**) caused relatively small shielding of 5-H.

Suitable crystals of **5aNO$_2$** were grown and its X-ray structure was determined (Figure 6 and Exp. Sect.). Nitro substitution at the bay-region resulted in minor distortion of the aromatic periphery (by 5.3°). The average dihedral angle between the NO_2 group and the PAH skeleton in this compound is 75.2°.

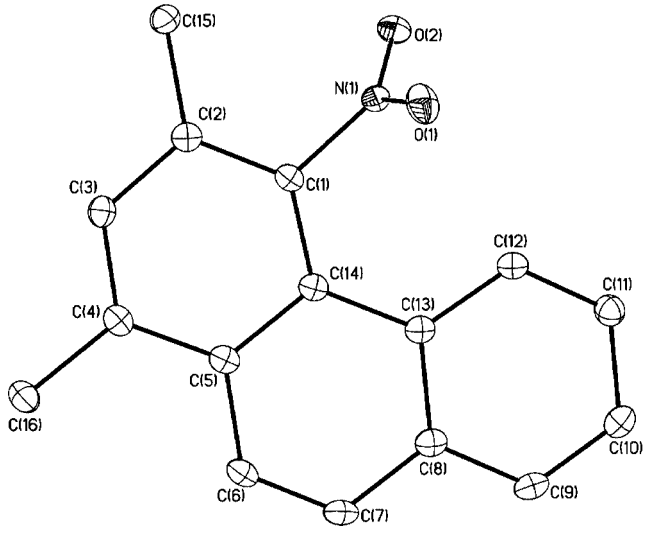

Figure 6. Thermal ellipsoid plot of **5aNO$_2$**. Ellipsoids are drawn at the 30% level.

d) DNA Binding Study

The nitro derivatives **1aNO$_2$**, **1bNO$_2$**, **3NO$_2$**, **4NO$_2$**, and **5bNO$_2$**, which were available as single isomers in high purity, were subjected to DNA binding study using human breast cancer cell line MCF-7. Reported results are based on one treatment of MCF-7 cells with 5 μM final concentration of each compound, after two replicates were postlabeled. Table 1 (see Exp. Sect.) summarizes the DNA adducts as pmol/mg of DNA (for further details on the procedures and protocols refer to experimental section). Although parent **9NPh** and **1NPh** were shown previously to be mutagenic in certain Salmonella strains,[4] the mononitro derivatives **1aNO$_2$** (nitro at C-9 in K-region), and **4NO$_2$** (nitro at C-1, *peri* to K-region) with a buttressed nitro group (as determined by X-ray) did not exhibit any measurable binding affinity to MCF cells in the present study. Compound **1bNO$_2$** with a nitro group in the bay-region exhibited low levels of binding to DNA. The mononitro derivative **5bNO$_2$** and the dinitro derivative **3NO$_2$** were both active, with the former showing the best defined peak in

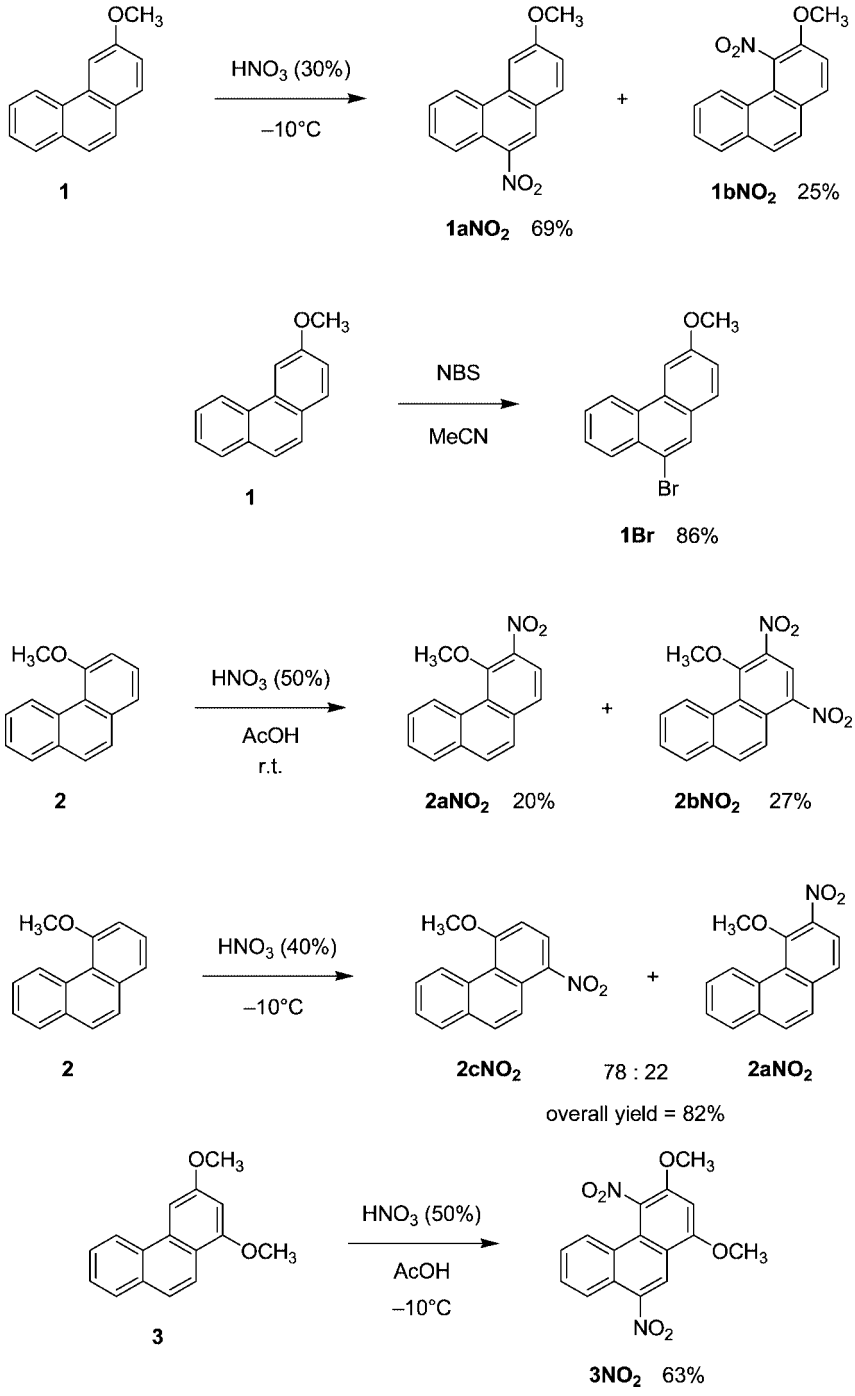

Scheme 2.

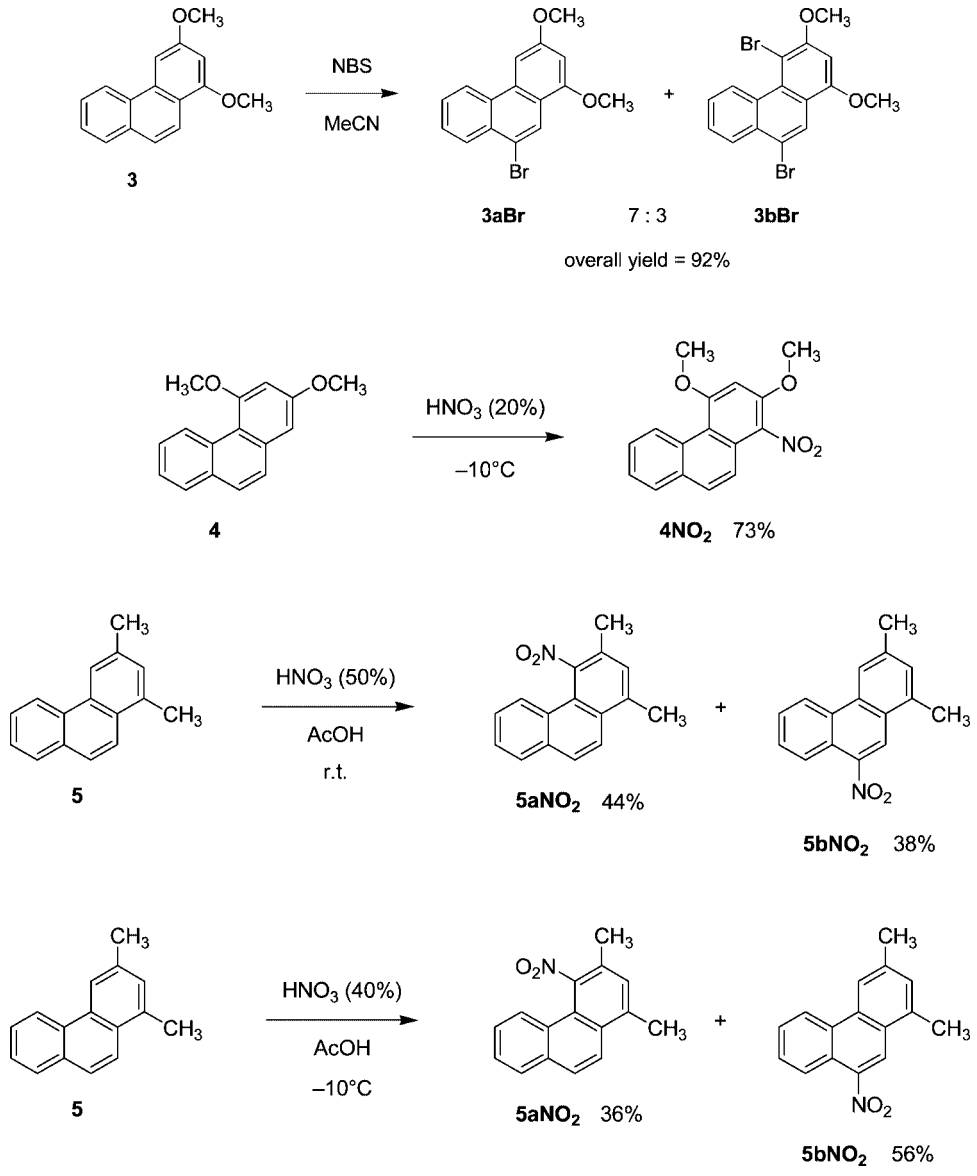

Scheme 2. *(continued)*

HPLC for the PAH-DNA adducts. Given that parent **4,9-diNPh** itself is very weakly mutagenic,[4] it appears that presence of activating substituents in the A-ring increased bio-activity.

Mutagenicity of nitro-phenanthrenes were previously correlated with the degree of out-of-plane bending of the nitro group and the LUMO energies (calculated by AM1).[4] To gain some insight into the effect of A-ring substitution in the present study, HOMO–LUMO energies were calculated by DFT [at the B3LYP/6-31G(d) level; see Supporting Information].

The HOMO and LUMO energies are lowered in going from **4NPh** to **9NPh** to **4,9-diNPh** (with the energy gap decreasing somewhat in the sequence). Methoxy substitution at C-3 (**1aNO$_2$**) increased the HOMO and LUMO energies (relative to **9NPh**) (with the gap decreasing somewhat). This effect was smaller for **5bNO$_2$** (HOMO is somewhat raised and LUMO remains relatively unchanged). Comparing **4,9-diNPh** with **3NO$_2$**, indicates that methoxy substitution at C-1/C-3 has a more pronounced affect on raising the HOMO and LUMO energies (with the gap decreasing overall). A similar comparison between **1bNO$_2$** and **4NPh** shows notable effects in raising the HOMO and LUMO energies by methoxy-substitution at C-3 (the gap remaining relatively unchanged).

Considering that nitro reduction and ring oxidation are both proposed as the main metabolic pathways for nitrophenanthrenes,[4] the present comparisons imply that among the nitro derivatives that exhibited DNA binding in this study, **3NO$_2$** and **1bNO$_2$** are less likely to metabolize via nitro-reduction as compared to their unsubstituted analogs.

Comparative Discussion

The presence of methoxy and methyl substituent(s) in the A-ring, coupled with their strong directive effects, was

shown to have a profound effect on the regioselectivity of carbocation formation. All five substrates were protonated in the A-ring. The resulting phenanthrenium ions exhibited rather similar charge delocalization patterns with positive charge strongly delocalized in the A-ring and limited delocalization through other rings. The carbocations could serve as models for epoxide ring opening in bay-region diol epoxides.

It is known, based on environmental studies, that phenanthrene and its derivatives are among the more prevalent components.[3] Extremely fast nitration of the A-ring substituted phenanthrenes, even in weak aqueous nitric acid as found in the present model study, infers that if this class of compounds finds its way into the environment, there is strong likelihood that the potentially toxic nitro derivatives could result.

There is very good overall correspondence between the low-temperature protonation study and the regioselectivity observed in mild aqueous nitration. In most reactions, two nitro products were obtained, one of them arising from a common type of carbocation intermediate as protonation, and the other likely arising from a higher energy regioisomeric carbocation or by further nitration of the initial product. In compound **4** identical regioselectivity was observed in protonation and nitration. With bromination, steric control of regioselectivity is much more significant, but nevertheless bay-region bromination, as observed in **3bBr**, reflects the highly favorable carbocation stabilizing effects of the 1,3-dimethoxy substituents. The X-ray structures of **4NO$_2$** and **5aNO$_2$** indicated that in both cases the nitro group is severely buttressed. In line with previous observations that nitrophenanthrenes with nitro group forced out of coplanarity exhibit low or no activity (presumably because they are unable to intercalate into DNA);[4] **4NO$_2$** did not exhibit DNA binding activity. Although only a limited set of compounds was studied for DNA binding, it appears that the methoxy and methyl substituents increase bioactivity in the nitro derivatives, and consideration of HOMO/LUMO energies suggests that the tendency for nitro-reduction as a main metabolic pathway has diminished in the case of **3NO$_2$** and **1bNO$_2$** relative to their unsubstituted nitro derivatives.

Experimental Section

General: Room temperature NMR spectra were recorded with a Bruker Avance 400 or a Varian 500 INOVA instrument. Low temperature NMR spectra were recorded exclusively with the Varian 500 INOVA with CD_2Cl_2 as NMR solvent. Electrospray-MS (ES-MS) data were acquired with a Bruker Esquire-LC instrument. Samples were prepared by addition of the compounds (10 μM) to AgOTs (30 μM) in MeOH.[11] Because of the existence of two stable isotopes for both silver and bromine atoms, only the averaged *m*/*z* values are reported. IR spectra were recorded with a Bruker Vector 33 instrument with Fourier Transform.

FSO_3H was distilled twice under argon in an all-glass distillation apparatus at atmospheric pressure and stored under argon at –20 °C in Nalgene bottles with Teflon seals. SO_2ClF was prepared according to a modified procedure of Prakash et al.[12]

Stable Carbocations Generation

Sample Preparation: In a 5-mm NMR tube was introduced the phenanthrene derivative (10–20 mg). The NMR tube was then flushed with argon, cooled to dry ice–acetone temperature and SO_2ClF (ca. 0.3 mL) was directly condensed into the NMR tube. After completion of SO_2ClF addition, 4–5 drops of FSO_3H were carefully added to minimize local overheating. The mixture immediately changed color, depending on the substitution pattern in the substrate (yellow-orange for methoxylated phenanthrenes and red for the dimethylated substrate). After vigorous stirring at –78 °C (vortex), 3–4 drops of CD_2Cl_2 were slowly introduced into the NMR tube (vortex mixing).

Quenching Procedure: The superacidic solution was carefully poured into a cold aqueous solution of sodium hydrogencarbonate, and then extracted three times with dichloromethane. The organic extract was dried with magnesium sulfate, filtered, concentrated under reduced pressure and the resulting solid residue was checked by ^{1}H NMR spectroscopy. In all cases, skeletally intact substrates were recovered upon quenching.

Nitration of 3-Methoxyphenanthrene (1): HNO_3 (1 mL, 30%) was added to a solution of **1** (30 mg, 0.14 mmol) in a 1:1 mixture of CH_2Cl_2/toluene (1 mL) at –10 °C (NaCl–ice bath). After 30 min of stirring, the reaction mixture was quenched with a saturated solution of $NaHCO_3$, whereupon two phases were separated. The aqueous phase was washed with CH_2Cl_2 (3 × 4 mL) and the combined organic extracts were dried with $MgSO_4$, filtered and evaporated under reduced pressure. The two isomers **1aNO$_2$** and **1bNO$_2$** thus obtained were separated and purified by preparative TLC using a CH_2Cl_2/hexane mixture (1:1).

3-Methoxy-9-nitrophenanthrene (1aNO$_2$): Yellow solid, 25 mg (69%). ^{1}H NMR (400 MHz, $CDCl_3$): δ = 8.59 (m, 1 H, 5-H), 8.57 (m, 1 H, 8-H), 8.44 (s, 1 H, 10-H), 7.94 (d, *J* = 2.4 Hz, 1 H, 4-H), 7.86 (d, *J* = 8.8 Hz, 1 H, 1-H), 7.68–7.74 (m, 2 H, 6,7-H), 7.29 (dd, *J* = 8.8, 2.4 Hz, 1 H, 2-H), 4.04 (s, 3 H, OCH_3) ppm. ^{13}C NMR (101 MHz, $CDCl_3$): δ = 161.3 (C-3), 143.5 (C-9), 134.1 (C), 132.1 (CH), 130.3 (C), 128.5 (CH), 127.5 (CH), 126.1 (CH), 124.1 (CH), 123.7 (C), 123.2 (C), 123.0 (CH), 118.2 (C-2), 104.2 (C-4), 55.6 (OCH_3) ppm. IR (CCl_4): $\tilde{\nu}$ = 2961, 1618, 1532 (NO), 1344 (NO), 1231 cm^{-1}. ES-MS (ESI+): *m*/*z* = 614 [M_2 + Ag]$^+$, 361 [M + Ag]$^+$.

3-Methoxy-4-nitrophenanthrene (1bNO$_2$): Yellow solid, 9 mg (25%). ^{1}H NMR (500 MHz, $CDCl_3$): δ = 8.24 (dm, *J* = 8.5 Hz, 1 H, 5-H), 7.96 (d, *J* = 8.8 Hz, 1 H, 1-H), 7.89 (dd, *J* = 8.0, 1.5 Hz, 1 H, 8-H), 7.69 (d, *J* = 9.0 Hz, 1 H, 10-H or 9-H), 7.66 (d, *J* = 9.0 Hz, 1 H, 9-H or 10-H), 7.64 (ddd, *J* = 8.0, 7.0, 1.2 Hz, 1 H, 7-H), 7.58 (ddd, *J* = 8.5, 7.0, 1.5 Hz, 1 H, 6-H), 7.38 (d, *J* = 8.8 Hz, 1 H, 2-H), 4.04 (s, 3 H, OCH_3) ppm. ^{13}C NMR (126 MHz, $CDCl_3$): δ = 149.9 (C-3), 133.6 (C), 131.5 (CH), 129.2 (CH), 127.9 (CH), 127.3 (CH), 126.9 (CH), 126.1 (CH), 125.6 (C), 123.9 (CH), 121.7 (C), 112.2 (C-2), 57.1 (OCH_3) ppm. IR (KBr): $\tilde{\nu}$ = 3018, 2938, 1604, 1528 (NO), 1372 (NO), 1280 cm^{-1}. ES-MS (ESI+): *m*/*z* = 614 [M_2 + Ag]$^+$, 361 [M + Ag]$^+$.

Nitration of 4-Methoxyphenanthrene (2)

Procedure A: AcOH (0.2 mL) and HNO_3 50% (0.2 mL) were added to a solution of **2** (38 mg, 0.18 mmol) in CH_2Cl_2 (1 mL). The reaction mixture was stirred overnight at room temperature. The mixture was quenched with a saturated solution of $NaHCO_3$. Two phases were separated, and the aqueous phase was washed with CH_2Cl_2 (3 × 4 mL). The combined organic layers were dried with

$MgSO_4$, filtered and evaporated under reduced pressure. The purification by preparative TLC of the resulting extract yielded 9 mg (20%) of the pale yellow solid **2aNO$_2$** and 14 mg (27%) of the dinitrated product **2bNO$_2$**.

Procedure B: HNO_3 (0.5 mL, 40%) was added to a solution of **2** (10 mg, 0.05 mmol) in CH_2Cl_2 (0.5 mL) at –10 °C (NaCl–ice bath). After 30 min of stirring, the reaction mixture was quenched with a saturated solution of $NaHCO_3$. Following the separation of the two phases, and the aqueous phase was washed with CH_2Cl_2 (3 × 3 mL). The combined organic layers were dried with $MgSO_4$, filtered and evaporated under reduced pressure. The resulting extract was purified by preparative TLC with a 1:1 mixture of CH_2Cl_2/hexane, giving 10 mg (82%) of a 78:22 mixture of the two regioisomers **2cNO$_2$** and **2aNO$_2$** respectively.

4-Methoxy-3-nitrophenanthrene (2aNO$_2$): ^{1}H NMR (400 MHz, $CDCl_3$): δ = 9.49 (dm, J = 8.4 Hz, 1 H, 5-H), 7.95 (dd, J = 8.0, 1.6 Hz, 1 H, 8-H), 7.93 (d, J = 8.8 Hz, 1 H, 2-H or 9-H), 7.89 (d, J = 8.8 Hz, 1 H, 9-H or 2-H), 7.73 (dm, J = 1.6 Hz, 1 H, 6-H), 7.73 (d, J = 8.8 Hz, 2 H, 1,10-H), 7.69 (ddm, J = 8.0, 7.2 Hz, 1 H, 7-H), 4.01 (s, 3 H, OCH_3) ppm. ^{13}C NMR (101 MHz, $CDCl_3$): δ = 152.8 (C-4), 136.9 (C-3), 133.0 (C-10a or C-4b), 131.0 (CH), 129.7 (C-4b or C-10a), 128.9 (CH), 128.0 (CH), 127.6 (CH), 127.5 (CH), 126.3 (CH), 124.9 (CH), 124.5 (C-8a), 121.8 (CH), 120.0 (C-4a), 62.2 (OCH_3) ppm. ES-MS (ESI+): m/z = 614 [M_2 + Ag]$^+$, 361 [M + Ag]$^+$.

4-Methoxy-1,3-dinitrophenanthrene (2bNO$_2$):[13] ^{1}H NMR (500 MHz, $CDCl_3$): δ = 9.48 (dm, J = 8.5 Hz, 1 H, 5-H), 8.58 (s, 1 H, 2-H), 8.28 (d, J = 9.5 Hz, 1 H, 10-H), 8.10 (d, J = 9.5 Hz, 1 H, 9-H), 8.01 (dm, J = 7.5 Hz, 1 H, 8-H), 7.82 (ddm, J = 7.5, 2.0 Hz, 1 H, 7-H), 7.79 (dm, J = 7.5 Hz, 1 H, 6-H), 4.05 (s, 3 H, OCH_3) ppm. IR (KBr): $\tilde{\nu}$ = 3091, 2940, 1605, 1518 (NO), 1349 (NO), 1248 cm^{-1}. ES-MS (ESI+): m/z = 704 [M_2 + Ag]$^+$, 406 [M + Ag]$^+$.

4-Methoxy-1-nitrophenanthrene (2cNO$_2$): ^{1}H NMR (400 MHz, $CDCl_3$): δ = 9.60 (dm, J = 8.4 Hz, 1 H, 5-H), 8.42 (d, J = 9.2 Hz, 1 H, 10-H), 8.26 (d, J = 9.0 Hz, 1 H, 2-H), 7.96 (d, J = 9.2 Hz, 1 H, 9-H), 7.94 (m, 1 H, 8-H), 7.65–7.73 (m, 2 H, 6,7-H), 7.13 (d, J = 9.0 Hz, 1 H, 3-H), 4.23 (s, 3 H, OCH_3) ppm. ^{13}C NMR (101 MHz, $CDCl_3$): δ = 162.5 (C-4), 141.3 (C-1), 132.3 (C), 131.6 (CH), 129.3 (C), 128.6 (CH), 128.5 (CH), 127.5 (CH), 127.1 (CH), 125.1 (CH), 121.2 (C), 120.2 (C-10), 120.0 (C-4a), 106.1 (C-3), 56.3 (OCH_3) ppm.

1,3-Dimethoxy-4,9-dinitrophenanthrene (3NO$_2$): AcOH (0.5 mL) and HNO_3 50% (0.5 mL) were added to a solution of **3** (52 mg, 0.22 mmol) in CH_2Cl_2 (2 mL) at –10 °C (NaCl–ice bath). After 10 min of stirring at –10 °C, the mixture was quenched with a saturated solution of $NaHCO_3$. A yellow precipitate was formed in the organic layer. Following the separation of two phases, the precipitate from the organic layer was filtered off. After drying the precipitate under vacuum, 41 mg of the pure yellow powder **3NO$_2$** were obtained. Subsequently, the combined organic phases were dried with $MgSO_4$, filtered and evaporated under reduced pressure. The rest of the product was purified by preparative TLC, using a 1:1 mixture of CH_2Cl_2/hexane, yielding overall 45 mg (63%) of a yellow powder. ^{1}H NMR (400 MHz, $CDCl_3$): δ = 8.92 (s, 1 H, 10-H), 8.51 (d, J = 8.4 Hz, 1 H, 5-H), 8.26 (d, J = 8.8 Hz, 1 H, 8-H), 7.79 (m, 1 H, 6-H), 7.67 (m, 1 H, 7-H), 6.81 (s, 1 H, 2-H), 4.16 (s, 3 H, OMe), 4.10 (s, 3 H, OMe) ppm. ^{13}C NMR (101 MHz, $CDCl_3$/CD_3CN): δ = 154.2, 153.3 (C-1,3), 129.4 (CH), 128.0 (CH), 124.4 (CH), 123.7 (CH), 119.0 (CH), 93.8 (C-2), 57.0 (OCH_3), 56.5 (OCH_3) ppm (C-4, C-4a, C-4b, C-8a, C-9 and C-10a were not detected). IR (KBr): 3096, 2955, 1614, 1514 (NO), 1356 (NO), 1220 cm^{-1}. ES-MS (ESI+): m/z = 764 [M_2 + Ag]$^+$, 436 [M + Ag]$^+$.

2,4-Dimethoxy-1-nitrophenanthrene (4NO$_2$): (ORTEP diagram, Figure 5) HNO_3 (1 mL, 20%) was added to a solution of **4** (46 mg, 0.19 mmol) in a mixture of CH_2Cl_2/toluene (1:1, 2 mL) at –10 °C (NaCl–ice bath). The mixture turned brown and dark. After 2 h of stirring, the reaction mixture was quenched with a saturated solution of $NaHCO_3$. Following the separation of two phases, the aqueous phase was washed with CH_2Cl_2 (3 × 4 mL). The combined organic layers were dried with $MgSO_4$, filtered and evaporated under reduced pressure. The product was then purified by preparative TLC using a 1:1 mixture of CH_2Cl_2/hexane. The resulting pure yellow solid was recrystallized from MeOH, yielding 40 mg (73%) of yellow crystals. ^{1}H NMR (400 MHz, $CDCl_3$): δ = 9.44 (dm, J = 8.8 Hz, 1 H, 5-H), 7.86 (dd, J = 8.0, 1.6 Hz, 1 H, 8-H), 7.84 (d, J = 9.0 Hz, 1 H, 9-H), 7.65 (ddd, J = 8.8, 7.2, 1.6 Hz, 1 H, 6-H), 7.58 (ddm, J = 8.0, 7.2 Hz, 1 H, 7-H), 7.53 (d, J = 9.0 Hz, 1 H, 10-H), 6.78 (s, 1 H, 3-H), 4.15 (s, 3 H, OCH_3), 4.04 (s, 3 H, OCH_3) ppm. ^{13}C NMR (101 MHz, $CDCl_3$): δ = 161.1 (C-4), 149.5 (C-2), 131.6 (CH), 131.4 (C-1), 129.4 (C), 128.7 (CH), 127.7 (CH), 127.6 (CH), 126.8 (C), 126.1 (CH), 118.6 (C-10), 114.8 (C-4a), 94.1 (C-3), 56.7 (OCH_3), 56.1 (OCH_3) ppm.

Nitration of 1,3-Dimethylphenanthrene (5)

Procedure A: AcOH (0.1 mL) and HNO_3 50% (0.1 mL) were added to a solution of **5** (15 mg, 0.07 mmol) in CH_2Cl_2 (0.5 mL). The reaction mixture was stirred overnight at room temperature. The mixture was quenched with a saturated solution of $NaHCO_3$. Then the two phases were separated and the aqueous layer was washed with CH_2Cl_2 (3 × 3 mL). The combined organic layers were dried with $MgSO_4$, filtered and evaporated under reduced pressure. The purification by preparative TLC of the resulting extract, using a 4:6 mixture of CH_2Cl_2/hexane, yielded 8 mg (44%) of **5aNO$_2$** and 7 mg (38%) of **5bNO$_2$**.

Procedure B: AcOH (0.2 mL) and HNO_3 40% (0.2 mL) were added to a solution of **5** (16 mg, 0.08 mmol) in CH_2Cl_2 (1 mL). The reaction mixture was stirred 1 h at –10 °C (NaCl–ice bath). The mixture was quenched with a saturated solution of $NaHCO_3$. Following the separation of the two phases, the aqueous phase was washed with CH_2Cl_2 (3 × 3 mL). The combined organic layers were dried with $MgSO_4$, filtered and evaporated under reduced pressure. The purification by preparative TLC of the resulting extract, using a 4:6 mixture of CH_2Cl_2/hexane, yielded 7 mg (36%) of **5aNO$_2$** and 11 mg (56%) of **5bNO$_2$**.

1,3-Dimethyl-4-nitrophenanthrene (5aNO$_2$): (ORTEP diagram, Figure 6) Pale orange solid. ^{1}H NMR (400 MHz, $CDCl_3$): δ = 8.26 (dm, J = 8.8 Hz, 1 H, 5-H), 7.92 (dd, J = 8.2, 1.6 Hz, 1 H, 8-H), 7.91 (d, J = 9.2 Hz, 1 H, 10-H), 7.81 (d, J = 9.2 Hz, 1 H, 9-H), 7.63 (ddd, J = 8.2, 7.2, 1.2 Hz, 1 H, 7-H), 7.58 (ddd, J = 8.8, 7.2, 1.6 Hz, 1 H, 6-H), 7.35 (s, 1 H, 2-H), 2.75 (s, 3 H, C^1CH_3), 2.49 (s, 3 H, C^3CH_3) ppm. ^{13}C NMR (101 MHz, $CDCl_3$): δ = 147.1 (C-4), 137.1 (C-1), 133.0 (C-8a), 130.6 (C-10a), 130.0 (C-2), 129.1 (C-8), 128.3 (C-9), 128.0 (C-3), 127.5 and 127.4 (C-7,6), 126.5 (C-4b), 124.1 (C-5), 122.0 (C-10), 120.9 (C-4a), 20.3 (C^1CH_3), 17.9 (C^3CH_3) ppm. ES-MS (ESI+): m/z = 610 [M_2 + Ag]$^+$, 359 [M + Ag]$^+$.

1,3-Dimethyl-9-nitrophenanthrene (5bNO$_2$): Yellow solid. ^{1}H NMR (400 MHz, $CDCl_3$): δ = 8.71 (m, 1 H, 5-H), 8.65 (s, 1 H, 10-H), 8.52 (m, 1 H, 8-H), 8.30 (s, 1 H, 4-H), 7.69–7.75 (m, 2 H, 6,7-H), 7.35 (s, 1 H, 2-H), 2.73 (s, 3 H, C^1CH_3), 2.60 (s, 3 H, C^3CH_3) ppm. ^{13}C NMR (101 MHz, $CDCl_3$): δ = 144.8 (C-9), 140.1 and 137.1 (C-1,3), 132.7 (C), 131.2 (C), 130.9 (CH), 128.1 (CH), 127.7 (CH), 125.9 (C), 123.8 (CH), 123.3 (CH), 123.1 (C), 122.0 (CH), 120.8 (CH), 22.3 (CH_3), 19.5 (CH_3) ppm. IR (KBr): $\tilde{\nu}$ = 3098, 2922, 1616,

1511 (NO), 1317 (NO) cm^{-1}. ES-MS (ESI+): *m/z* = 610 $[M_2 + Ag]^+$, 359 $[M + Ag]^+$.

Electrophilic Bromination Reactions. General Procedure: A solution of *N*-bromosuccinimide (0.12 mmol) in acetonitrile (1 mL) was added to a solution of the substrate (0.1 mmol) in acetonitrile (1 mL). The mixture was stirred at room temperature during 10–15 h, washed with brine (2 mL) and extracted with dichloromethane (3 × 3 mL). The recombined organic layer was dried with magnesium sulfate, filtered and evaporated under reduced pressure. The brominated compound was then purified by either column chromatography or preparative TLC.

9-Bromo-3-methoxyphenanthrene (1Br): White solid, 26 mg (86%). ^{1}H NMR (400 MHz, $CDCl_3$): δ = 8.58 (m, 1 H, 5-H), 8.35 (m, 1 H, 8-H), 8.02 (s, 1 H, 10-H), 7.98 (d, *J* = 2.4 Hz, 1 H, 4-H), 7.70 (d, *J* = 8.8 Hz, 1 H, 1-H), 7.65–7.70 (m, 2 H, 6,7-H), 7.23 (dd, *J* = 8.8, 2.4 Hz, 1 H, 2-H), 4.01 (s, 3 H, OCH_3) ppm. ^{13}C NMR (101 MHz, $CDCl_3$): δ = 158.7 (C-3), 131.1 (C-4a), 130.7 and 130.6 (C-4b,8a), 130.1 (C-10), 129.2 (C-1), 128.0 (C-8), 127.5 (C-7), 126.9 (C-6), 126.6 (C-10a), 122.8 (C-5), 118.8 (C-9), 117.3 (C-2), 104.1 (C-4), 55.5 (OCH_3) ppm. IR (KBr): $\tilde{\nu}$ = 3067, 2931, 1618, 1501 (NO), 1369 (NO), 1214, 747 (CBr) cm^{-1}. ES-MS (ESI+): *m/z* = 682 $[M_2 + Ag]^+$, 395 $[M + Ag]^+$.

Bromination reaction performed on **3** led, after purification by preparative TLC, to 38 mg (92%) of a 7:3 mixture of the monobrominated product **3aBr** and the dibrominated product **3bBr**, respectively, which were analyzed as a mixture. ES-MS (ESI+): *m/z* = 900 $[Mb – Ag – Mb]^+$, 821 $[Ma – Ag – Mb]^+$, 742 $[Ma – Ag – Ma]^+$, 504 $[Mb – Ag]^+$, 425 $[Ma – Ag]^+$.

9-Bromo-1,3-dimethoxyphenanthrene (3aBr): ^{1}H NMR (500 MHz, $CDCl_3$): δ = 8.53 (dm, *J* = 8.5 Hz, 1 H, 5-H), 8.46 (s, 1 H, 10-H), 8.33 (dm, *J* = 8.0 Hz, 1 H, 8-H), 7.61–7.72 (m, 2 H, 6,7-H), 7.52 (d, *J* = 2.2 Hz, 1 H, 4-H), 6.62 (d, *J* = 2.2 Hz, 1 H, 2-H), 3.99 (s, 3 H, OMe), 3.98 (s, 3 H, OMe) ppm. ^{13}C NMR (126 MHz, $CDCl_3$): δ = 159.3 and 156.3 (C-3,1), 124.3 (C-10), 123.2 (C-5), 98.3 (C-2), 95.3 (C-4) ppm.

4,9-Dibromo-1,3-dimethoxyphenanthrene (3bBr): ^{1}H NMR (500 MHz, $CDCl_3$): δ = 9.95 (dm, *J* = 8.5 Hz, 1 H, 5-H), 8.43 (s, 1 H, 10-H), 8.35 (m, 1 H, 8-H), 7.61–7.72 (m, 2 H, 6,7-H), 6.70 (s, 1 H, 2-H), 4.02 (s, 3 H, C^3OCH_3), 3.99 (s, 3 H, C^1OCH_3) ppm. ^{13}C NMR (126 MHz, $CDCl_3$): δ = 156.2 and 155.4 (C-3,1), 128.0 (C-5), 123.9 (C-10), 94.7 (C-2) ppm.

DNA Binding Study. Cell Culture and Treatment: The MCF-7 cells (Karmanos Cancer Center, Detroit, MI) were cultured in a 75-cm^2 flask (Corning, Corning, NY) in a 1:1 mixture of F-12 Nutrient Mixture and Dulbecco's Modified Eagle's Medium (DMEM; Gibco BRL, Grand Island, NY) and 10% fetal bovine serum (Intergen, Purchase, NY) at 37 °C with 5% CO_2. The media contained 15 mM HEPES buffer and sodium hydrogencarbonate. Each compound was added to 80% confluent cells in 20 mL fresh media at a final concentration of 1 or 5 μM. After 24 h, the cells were harvested by trypsin, washed in PBS and kept at –80 °C until needed for DNA isolation.

DNA Isolation: MCF-7 cell pellets from two T 75 flasks per treatment were homogenized in lysis buffer (10 mM Tris, 1 mM Na_2EDTA, 1% SDS, pH 8). The homogenates were treated with RNase, DNase-free (50 U/mL) (Boehringer Mannheim Company, Indianapolis, IN) and RNase T1 (1000 U/mL) (Boehringer Mannheim) at 37 °C for 1 h, followed by treatment with proteinase K (500 μg/mL) (Sigma) at 37 °C for 1 h. The DNA was extracted in light Phase Lock Gel tubes (Eppendorf AG, Hamburg, Germany) with equal volumes of Tris-equilibrated phenol (Boehringer Mannheim) and chloroform/isoamyl alcohol (24:1). The DNA was precipitated in ethanol and its oncentration was determined by UV absorbance at 260 nm.

^{33}P-Postlabeling of DNA Adducts: 10 μg DNA isolated from MCF-7 cells after treatment were digested with nuclease P1 (0.4 U, Sigma) and prostatic acid phosphatase (350 mU, Sigma) and radiolabeled by T4 polynucleotide kinase (18 U, USB Corporation), and γ-^{33}P-ATP (5 μCi, 3,000 Ci/mmol, Perkin–Elmer). The ^{33}P-labeled samples were digested with snake venom phosphodiesterase (15 mU, USB) and apyrase (100 mU, Sigma).[14] The postlabeled samples were cleaned to remove unbound ^{33}P prior to HPLC analysis on a Sep-Pak C_{18} cartridge (Waters) and eluted in 2 mL of methanol and ammonium hydroxide (95:5). The radioactivity of samples was determined by liquid scintillation counting (Packard Instruments) and one million counts were analyzed by HPLC. The amount of adducts was calculated based on the postlabeling efficiency of [1,3-^{3}H]-(+)-(7*R*)-*r*-7,*t*-8-Dihydroxy-*t*-9,10-epoxy-7,8,9,10-tetrahydrobenzo[*a*]pyrene purchased from National Cancer Institute's Chemical Carcinogen Reference Standard Repository.

HPLC Analysis: Gradient from 0 to 40% B in 20 min, to 80% in 30 min, to 90% in 35 min, to 0% B at 45 min which was the total run time. Buffer A was 0.05 M $NH_4H_2PO_4$ in water, solvent B was methanol, and the flow rate was 1 mL/ min. The column used was Beckman C-18, 4.6 × 250 mm, 5 μ particle size, and the HPLC system was Varian Pro Star 210 equipped with Varian 420 autosampler. The peaks were detected with a 400 μL dry cell on a β-RAM® Model 3-HPLC Beta radioactive detector (Table 1).

Table 1. A = **1aNO$_2$**; B = **1bNO$_2$**; C = **3NO$_2$**; D = **4NO$_2$**; Z = **5bNO$_2$**.

Sample	DNA adducts (pmol/mg of DNA)	Sample	DNA adducts (pmol/mg of DNA)
La A	0	bp1	89.53294
a1	0	std2	378.938
La B	0	std1	448.9622
b1	13.56936	BP	78.63017
La C	28.08096	LaZ	0
c1	0	laZa	18.19811
La D	0	LaDMSO	3.479961
d1	0.365329	LaBPa	57.7566
BP	0		

X-ray Crystallographic Data: X-ray crystallography was performed by mounting each crystal onto a thin glass fiber from a pool of Fluorolube™ and immediately placing it under a liquid N_2 stream, on a Bruker AXS diffractometer. The radiation used was graphite-monochromatized Mo-K_α radiation (λ = 0.7107 Å). The lattice parameters were optimized from a least-squares calculation on carefully centered reflections. Lattice determination, data collection, structure refinement, scaling, and data reduction were carried out using APEX2 version 1.0–27 software package. Each structure was solved by direct methods. This procedure yielded a number of the C, N, and O atoms. Subsequent Fourier synthesis yielded the remaining atom positions. The hydrogen atoms were fixed in positions of ideal geometry and refined within the XSHELL software. These idealized hydrogen atoms had their isotropic temperature factors fixed at 1.2 or 1.5 times the equivalent isotropic U of the C atoms to which they were bonded. The final refinement of each

compound included anisotropic thermal parameters on all non-hydrogen atoms.

Crystal Data for $4NO_2$: $C_{16}H_{13}NO_4$, M_w = 283.27 g mol^{-1}, crystal dimensions 0.15 × 0.10 × 0.09 mm, monoclinic, space group $P2_1/n$, a = 10.2113(10), b = 7.5656(8), c = 16.7368(17) Å, β = 95.356(2)°; V = 1287.3(2) Å^3, Z = 4, $\rho_{calcd.}$ = 1.462 g cm^{-3}, Bruker SMART APEX II diffractometer, 2.25 < θ < 25.25, Mo-K_α radiation (λ = 0.71073 Å), ω scans, T = 105(2) K; of 10083 measured reflections, 2324 were independent and 1910 observed with $I > 2\sigma(I)$, R_1 = 0.0316, wR_2 = 0.0979, GOF = 0.731 for 192 parameters, $\Delta\rho_{max}$ = 0.012 e Å^{-3}. The structure was solved by direct methods (SHELXS-97) and refined by full-matrix least-squares procedures (SHELXL-97), Lorentzian and polarization corrections and absorption correction SADABS were applied, μ = 0.106 mm^{-1}.

Crystal Data for $5aNO_2$: $C_{16}H_{13}NO_2$, M_w = 251.27 g mol^{-1}, crystal dimensions 0.20 × 0.15 × 0.10 mm, triclinic, space group $P\bar{1}$, a = 7.7881(11), b = 9.2769(13), c = 9.7062(13) Å, α = 63.706(2)°, β = 77.781(2)°; γ = 74.096(2)°, V = 601.32(14) Å^3, Z = 2, $\rho_{calcd.}$ = 1.388 g cm^{-3}, Bruker SMART APEX II diffractometer, 2.35 < θ < 25.25, Mo-K_α radiation (λ = 0.71073 Å), ω scans, T = 100(2) K; of 4937 measured reflections, 2177 were independent and 1900 observed; R_1 = 0.0314, wR_2 = 0.1050, GOF = 0.714 for 174 parameters, $\Delta\rho_{max}$ = 0.037 e Å^{-3}. The structure was solved by direct methods (SHELXS-97) and refined by full-matrix least-squares procedures (SHELXL-97), Lorentzian and polarization corrections and absorption correction SADABS were applied, μ = 0.092 mm^{-1}.

CCDC-619525 (for **$4NO_2$**) and -619524 (for **$5aNO_2$**) contain the supplementary crystallographic data for this paper. These data can be obtained free of charge from The Cambridge Crystallographic Data Centre via www.ccdc.cam.ac.uk/data_request/cif.

Supporting Information (see also the footnote on the first page of this article): Additional supporting data, namely representative ^{1}H/^{13}C NMR spectra for the carbocations, HOMO/LUMO energies, and HPLC profiles.

Acknowledgments

We are grateful to Prof. A. Fürstner and Dr. V. Mamane (Max-Planck Institute, Mülheim, Germany) for providing the A-ring substituted phenanthrenes (ref.[9]), and to Dr. Scott Bunge (KSU) for X-ray analysis. Support of our work by the NCI of NIH (2R15-CA078235-02A1) (project "reactive intermediates of carcinogenesis of PAHs") is also gratefully acknowledged.

[1] R. G. Harvey, *Polycyclic Aromatic Hydrocarbons; Chemistry and Carcinogenicity*, Cambridge Monographs on Cancer Research, Cambridge, **1991**.
[2] *Polycyclic Hydrocarbons and Carcinogenesis*, ACS Symposium Series 283 (Ed.: R. G. Harvey), ACS, Washington DC, **1985**.
[3] E. J. LaVoie, J. E. Rice, in *Polycyclic Aromatic Hydrocarbon Carcinogenesis: Structure-Activity Relationships* (Eds.: S. K. Yang, B. D. Silverman), CRC Press, Boca Raton, Florida, **1988**, vol. 1, chapter 6.
[4] a) N. Sera, K. Fukuhara, N. Miyata, H. Tokiwa, *Mutat. Res.* **1996**, *349*, 137–144; b) K. Fukuhara, M. Takei, H. Kageyama, N. Miyata, *Chem. Res. Toxicol.* **1995**, *8*, 47–54.
[5] K. Laali, H. Cerfontain, *J. Org. Chem.* **1983**, *48*, 1092–1095.
[6] K. K. Laali, S. Hollenstein, P. E. Hansen, *J. Chem. Soc., Perkin Trans. 2* **1997**, 2207–2213.
[7] K. K. Laali, J. E. Gano, C. W. Gundlach IV, D. Lenoir, *J. Chem. Soc., Perkin Trans. 2* **1994**, 2169–2173.
[8] K. K. Laali, T. Okazaki, S. Kumar, S. E. Galembeck, *J. Org. Chem.* **2001**, *66*, 780–788.
[9] A. Fürstner, V. Mamane, *J. Org. Chem.* **2002**, *67*, 6264–6267.
[10] R. M. Letcher, *Org. Magn. Reson.* **1981**, *16*, 220–223.
[11] K. K. Laali, S. Hupertz, A. G. Temu, S. E. Galembeck, *Org. Biomol. Chem.* **2005**, *3*, 2319–2326.
[12] V. P. Reddy, D. R. Bellew, G. K. S. Prakash, *J. Fluorine Chem.* **1992**, *56*, 195–197.
[13] S. Sekiguchi, M. Hirai, E. Ota, H. Hiratsuka, Y. Mori, S. Tanaka, *J. Org. Chem.* **1985**, *50*, 5105–5108.
[14] S. L. Ralston, H. H. S. Lau, A. Seidel, A. Luch, K. L. Platt, W. M. Baird, *Cancer Res.* **1994**, *54*, 887–890.

Received: September 5, 2006
Published Online: November 13, 2006

